

THE FATE OF THE COMPACT REMNANT IN NEUTRON STAR MERGERS

CHRIS L. FRYER^{1,2}, KRZYSZTOFF BELCZYNSKI³, ENRICO RAMIREZ-RUIZ⁴, STEPHAN ROSSWOG⁵, GANG SHEN⁶, ANDREW W. STEINER^{7, 8}

Draft version October 3, 2018

ABSTRACT

Neutron star (binary neutron star and neutron star - black hole) mergers are believed to produce short-duration gamma-ray bursts. They are also believed to be the dominant source of gravitational waves to be detected by the advanced LIGO and the dominant source of the heavy r-process elements in the universe. Whether or not these mergers produce short-duration GRBs depends sensitively on the fate of the core of the remnant (whether, and how quickly, it forms a black hole). In this paper, we combine the results of merger calculations and equation of state studies to determine the fate of the cores of neutron star mergers. Using population studies, we can determine the distribution of these fates to compare to observations. We find that black hole cores form quickly only for equations of state that predict maximum non-rotating neutron star masses below 2.3-2.4 solar masses. If quick black hole formation is essential in producing gamma-ray bursts, LIGO observed rates compared to GRB rates could be used to constrain the equation of state for dense nuclear matter.

Subject headings: Supernovae: General

1. INTRODUCTION

Since their discovery in the late 1970s (Klebesadel and Strong 1976), scientists have proposed a growing number of progenitors and engines for gamma-ray bursts (GRBs). The variety in the observations of classical GRBs points to multiple progenitor scenarios. Based on their duration, bursts are traditionally separated in long and short GRBs (Kouveliotou et al. 1993). Within the black hole accretion disk (BHAD) class of models, long-duration bursts are believed to arise from accreting black holes at the center of massive stars, e.g. from collapsars (Woosley 1993) or he-mergers (Fryer et al. 1999). Short-duration bursts are believed to be produced by the merger of two compact objects: consisting either of a binary neutron star (NS-NS) or a neutron star and a black hole (BH-NS): for review see, for example, Fryer et al. (1999); Popham et al. (1999); Lee and Ramirez-Ruiz (2007); Rosswog (2015). These compact mergers are produced in close binaries and the kicks imparted onto these compact remnants cause these systems to have high space velocities. These velocities, coupled with merger times, mean that bursts produced from NS-NS and BH-NS binaries should have broad spatial distributions with respect to their host galaxy, including bursts that occur well outside of their host (Bloom et al. 1999; Fryer et al. 1999;

Zemp et al. 2009). With Swift, the number of localized short-duration bursts has increased dramatically, and the observed spatial distributions of these bursts matches the predictions from theory (Belczynski et al. 2006; Fong and Berger 2013; Behroozi et al. 2014). Indeed, no other model to date can easily explain the spatial distributions of short-duration bursts, and NS-NS and BH-NS mergers are almost universally considered the leading progenitors for these bursts.

The BHAD engine is not the only way accreting compact objects can produce possible outflows. Neutron stars are also able to accrete at Super-Eddington rates (Houck and Chevalier 1991; Fryer et al. 1996) and NS accretion disk (NSAD) systems will look very similar to BHAD engines. Alternatively, building off of the leading mechanism for soft gamma-ray repeaters (SGR), theorists have argued that rapidly-spinning magnetars (Duncan and Thompson 1992) can produce classical GRBs (Zhang and Meszaros 2001). The disadvantage of the neutron star models is that they – as long as the merger remnant is stable – can drive strong baryonic winds via neutrino energy deposition (Dessart et al. 2009; Perego et al. 2014) that potentially choke the GRB jet (Rosswog and Ramirez-Ruiz 2002; Murguia-Berthier et al. 2014).

The advantage of the neutron star model is that the NS can be born with strong magnetic fields⁹ and these magnetars provide a means to drive late-time emission (Usov 1992; Thompson 1994; Rowlinson et al. 2014). Understanding the relative rate of merging systems that form black holes versus neutron stars can help direct theorists toward a better understanding of these systems. For example, if very few systems collapse to form black holes, either the baryonic loading problem is less severe than

¹ Department of Physics, The University of Arizona, Tucson, AZ 85721

² CCS Division, Los Alamos National Laboratory, Los Alamos, NM 87545

³ Astronomical Observatory, University of Warsaw, Al Ujazdowskie 4, 00-478 Warsaw, Poland

⁴ Department of Astronomy and Astrophysics, University of California, Santa Cruz, CA 95064

⁵ The Oskar Klein Center, Department of Astronomy, AlbaNova, Stockholm University, SE-106 91 Stockholm, Sweden

⁶ Institute for Nuclear Theory, University of Washington, Seattle, Washington 98195

⁷ Department of Physics and Astronomy, University of Tennessee, Knoxville, Tennessee 37996, USA

⁸ Physics Division, Oak Ridge National Laboratory, Oak Ridge, Tennessee 37831, USA

⁹ Note that generally in high accretion scenarios like these merger systems, there is a belief that the accretion buries the field (Popov and Turolla 2012; Vigano and Pons 2012). Typical timescales for the re-emergence of these magnetic fields are tens of kyr. In such a case, any magnetar-like model will not work to explain a GRB.

currently believed or mergers are not the solution to GRBs. On the other extreme, if only a small fraction remain neutron stars, it is worth identifying and trying to observe the failed GRBs formed by these systems. Observations of relative rates of these systems can provide a fairly direct means to constrain the nuclear equation of state.

This paper brings together studies of binary neutron star merger models, nuclear equations of state, and population synthesis models to study the formation rate of different potential GRB progenitors, differentiating between black hole accretion disk models, accretion-induced collapse models, and neutron star accretion models. Section 2 describes the merger models used in this study and Section 3 describes the effects and uncertainties in the equation of state (EOS). By coupling these results with population synthesis studies, we can compare these results to the suite of GRB observations (Section 4). We conclude with a discussion of the implications of these results on the wide range of phenomena explained by NS-NS and BH-NS binaries.

2. MERGER MODELS

In the past decade, the number of hydrodynamic simulations of NS-NS and BH-NS mergers has grown considerably (Foucart et al. 2010, 2011; Foucart 2012; Korobkin et al. 2012; Hokokezaka et al. 2013; Kyutoku et al. 2013; Takami et al. 2014; Bauswein et al. 2014; Radice et al. 2014; Shibata et al. 2014; Kiuchi et al. 2014; Foucart et al. 2015). Although these models are becoming increasingly sophisticated, most of the current models include only a subset of the physics needed to model these objects: hydrodynamics, neutrino transport (or at least neutrino energy losses), nuclear equations of state, magnetic fields, and general relativity. Nevertheless, these models are gradually painting a complete picture of the merger process and we can use them to make a first pass at the fate of these systems.

2.1. BH-NS mergers

To date, no BH-NS system has been observed and, at this point, there are no observations that would require such systems to exist. However, there are clear observational biases against such systems: if the NS is formed after the black hole, as we expect, it is difficult to recycle it. Hence we do not expect a millisecond pulsar in BH-NS binaries. Population synthesis models predict that these systems form frequently and many of them close enough to merge within a Hubble time. Theoretical models for massive star evolution and the formation of BH-NS systems suffer from large uncertainties (e.g., treatment of star internal mixing, stellar winds, common envelope and supernova explosion). Population synthesis models predict a range of formation rates from several orders of magnitude below the BNS merger rate to rates that rival the BNS rate (Dominik et al. 2012).

The binary parameters of BH-NS systems are crucial for the outcome of the merger and only for a fraction of the parameter space will it be possible to form an accretion disk massive enough to launch a GRB. If we assume the energy arises from the disk,

$$E_{\text{ext}} \sim 2 \times 10^{51} \text{ erg} \left(\frac{\epsilon}{0.1} \right) \left(\frac{M_{\text{disk}}}{0.01 M_{\odot}} \right) \quad (1)$$

can be extracted, so that the disks do not need to be extremely massive to accommodate the typical isotropic gamma-ray energies of short bursts (Berger 2014) of $\sim 10^{50}$ erg (and correspondingly lower if they are collimated). If the energy arises from the rotating black hole, significantly smaller disk masses are needed to produce the energies required for short bursts (Lee and Ramirez-Ruiz 2007). Nevertheless, not all systems will be able to form disks, since the radius where tidal disruption sets in, R_{tid} , must be larger than the innermost stable circular orbit (ISCO), R_{ISCO} . Since $R_{\text{ISCO}} \propto M_{\text{BH}}$, but $R_{\text{tid}} \propto M_{\text{BH}}^{1/3}$, for massive enough black holes the tidal radius lies inside of the ISCO and forming a massive accretion disk becomes impossible. For a non-spinning black hole this occurs already near $M_{\text{BH}} = 8 M_{\odot}$, so that BHs of the masses that are thought (Belczynski et al. 2008; Ozel et al. 2010) to be most likely ($\sim 10 M_{\odot}$) need large dimensionless spin parameters, $a_{\text{BH}} \gtrsim 0.9$, to form sizeable disks (Foucart 2012). Finally, the inclination of vector of BH-NS orbital angular momentum to BH spin vector plays an important role in the formation of a torus. At large inclination angles ($\gtrsim 40 - 90^{\circ}$), material from the disrupted NS is ejected from the vicinity of a merger and does not form torus. Non-zero tilts are expected in BH-NS systems if a NS is formed as a second compact object in a binary and with a non-zero natal kick in isolated binary evolution in field populations (Fryer et al. 1999; Dominik et al. 2012, 2013, 2014) and, in majority of cases, in dynamical evolution; e.g., globular clusters (Grindlay et al. 2006; Lee et al. 2010; East et al. 2013; Rosswog 2013; Tsang 2013; Ramirez-Ruiz et al. 2015).

The number of simulations studying these mergers and their fates has grown with time (Rosswog 2004, 2005; Rantsiou et al. 2008; Foucart et al. 2010, 2011; Kyutoku et al. 2013; Paschalidis et al. 2014; Foucart et al. 2015), all showing that the final fate of the merged system depends sensitively upon the initial conditions. Based on earlier merging BH-NS models by Rantsiou et al. (2008), it was shown for one particular evolutionary model that only a fraction of BH-NS systems may potentially form an accretion torus and lead to a GRB. For small BH spins ($a_{\text{spin}} < 0.6$), only 1% of BH-NS mergers were found to have a disk needed to produce a GRB. For high BH spins the fraction of systems with disks have been calculated to be $\sim 40\%$ Belczynski et al. (2008). It is important, that in future studies, the merger hydrodynamical simulations are mapped with astrophysically-motivated predictions of BH-NS system physical properties.

For this paper, we will assume the GRB rate is dominated by BNS mergers, but we will return to the topic of BH-NS mergers when we better understand the BNS results.

2.2. NS-NS mergers

NS-NS mergers always form sizable accretion disks and are the more canonical GRB model. The primary difficulty with these mergers as GRB progenitors is the nature of the merged core. After the merger, the remnant will evolve according to four separate pathways: collapse directly to black holes, those that initially form NSs but subsequently collapse during disk accretion, those that don't collapse to black holes until after the disk has fully

accreted and the newly formed neutron star spins down, and those that, even after the spin down, remain a NS. To determine the fate of each merged object, we must combine both simulations of the merger process (discussed in this section) with our current understanding of the nuclear equation of state (see Section 3). For two equally-massed neutron stars, the merger produces a condensed core consisting of two major components formed from the cores of the initial neutron stars. As the mass ratio becomes more extreme, the more massive neutron star remains more intact, disrupting its companion. In all cases, the merger produces a merged core surrounded by a dense accretion disk with a small amount of material ($\sim 1\%$) ejected during the tidal ejection process.

To study the fates of neutron stars, we use the large grid of smooth particle hydrodynamics simulations from Korobkin et al. (2012). This grid of models includes a broad suite of neutron star mass pairs using the same input physics. For each simulation, we calculate the mass and angular momentum of the merged core (all material above $10^{14} \text{ g cm}^{-3}$), disk masses (bound mass with densities below $10^{14} \text{ g cm}^{-3}$) and ejecta masses (Table 1).

At the end of the smooth particle hydrodynamics simulations, considerable mass ($\sim 0.5 - 0.9 M_{\odot}$) remains bound but at densities below $10^{14} \text{ g cm}^{-3}$. In Table 1, we refer to this material as “disk” material and much of it will form a disk that quickly accretes onto the compact core. If the core collapses to a black hole, the system immediately evolves into a BHAD engine. If not, it may first pass through a neutron star accretion disk or magnetar engine until the accretion drives the neutron star above the maximum mass and it collapses, producing a BHAD scenario.

Whether or not the core is a black hole or neutron star depends upon whether it is more massive than the maximum neutron star mass at its spin rate. This depends upon the still-uncertain equation of state. Recent observations by Demorest et al. (2010) and Antoniadis et al. (2013) demonstrate that this mass is least $2 M_{\odot}$. The exact value for the maximum mass of a particular merged core depends on the equation of state as well as the internal energy and angular momentum distribution in the core. Our choice of equation of state will determine which merged cores collapse immediately to a black hole.

In other cases, the core must accrete some material before it collapses. To determine the engine behind this neutron star, we must understand the accretion timescale. If the core remains a neutron star for a long period of time, the neutrino-driven wind will choke the outflow, preventing a strong burst (Murguía-Berthier et al. 2014). To estimate the accretion time of the disk, we use the matter distribution from our models and assume an α -driven disk scenario. That is, for the spatial distribution of the disk material, we assume the accretion timescale is just the orbital period divided by the value of α : $T_{\text{acc}} = \frac{1}{\alpha} \frac{2\pi r^{3/2}}{(GM_{\text{encl}})^{1/2}}$ where r is the spatial position of the matter, M_{encl} is the enclosed mass and α is the viscous disk parameter. Figure 1 shows the mass of the core as a function of time under our α -disk assumptions using $\alpha = 0.01$. Note that although much of the accretion occurs in the first 100 ms, the accretion phase can last out to a few seconds for some systems. Clearly, the

accretion time depends linearly on the value for α whose value is uncertain to an order of magnitude.

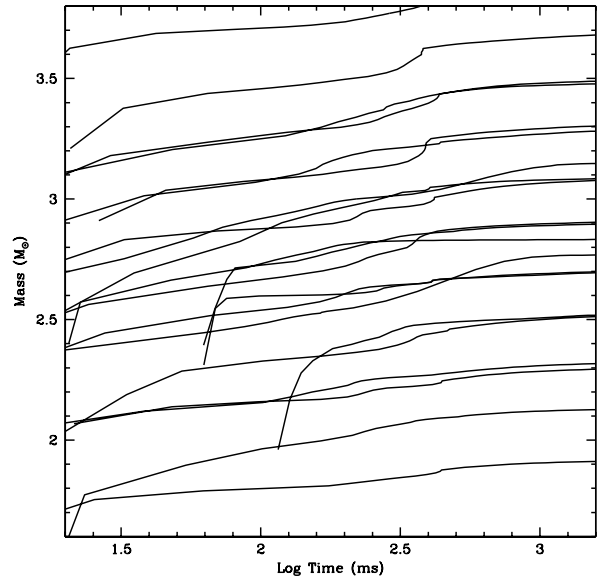


Figure 1. Core mass versus time for our merged systems assuming an α -disk solution for the accretion time. Note that in many systems, the accretion occurs very rapidly (in the first 10,ms) and can last out to a few seconds. The jumps occur because the angular momentum of material is not uniform and large amounts of material have similar angular momenta, and hence, accretion timescales.

For the most part, these models assume that the neutron stars in the binary are initially not spinning (although for one case, we include a neutron star binaries in co-rotation). The assumption is well-justified since the last inspiral stages happen so quickly that even an unphysically large dissipation cannot spin up the stars substantially (Bildsten & Cutler 1992; Kochanek 1992). Pre-merger spins are typically substantially smaller than co-rotation, but even in the co-rotation case, the mass is altered by only a few percent, but the angular momentum in the core can change by 15%. This has only a small affect on the maximum stable neutron star mass of the core, but it can dramatically change the accretion rate (see Section 3).

Be aware that the current set of simulations are incomplete, missing both physics and spatial resolution to model the physics. As this physics is improved, exact quantities on merged cores, etc. will move. But the basic trends will continue and, although there may be a shift in our results, the trends and methodology to study NS-NS and BH-NS mergers the results will remain.

3. EQUATION OF STATE

The fate of the core depends on the exact details of the equation of state. If the maximum neutron star mass were $2.0M_{\odot}$, the maximum observed neutron star mass (Demorest et al. 2010; Antoniadis et al. 2013), most of our merger cases would immediately collapse to a black hole. This observation only places a lower limit on the maximum mass, and the maximum mass of a cold neutron star may, depending upon the equation of state, be much higher than this maximum observed mass. In addition, fast-rotation and thermal energy can significantly raise the maximum mass. To determine the final fate of our merger remnants, we will study the maximum mass, and its dependence on the spin and internal energy, for a range of equation of state models.

The merged core, especially if the components are near-equal mass, are often born with strong differential rotation (Rosswog and Davies 2002). Depending upon the magnetic field strength, these cores will very quickly evolve into uniform rotation. For example, Shibata et al. (2007) argue that a combination of magnetic winding, shearing and the magnetorotational instability can quickly redistribute the angular momentum in an accreting disk system. For a few of our fastest rotating mergers (the merger of a $2.0 M_{\odot}$ NS with a $1.0, 1.2 M_{\odot}$ NS and the merger of a $1.8 M_{\odot}$ NS with a $1.0 M_{\odot}$ NS: see Table 1), secular instabilities can develop that will also redistribute the angular momentum. Finally, neutrino cooling in the core will drive convection in the core (Rosswog et al. 2003) that can redistribute the angular momentum. These redistribution mechanisms have timescales lying between 10-100 ms. If it is at the low end, our assumption that it is nearly instantaneous holds. If there is a longer delay in this evolution to uniform rotation, the maximum mass could remain high for longer, producing more long-lived neutron star systems. Note, however, that for our population study (see section 4), only 0.3% of our systems have a NS component with masses above $1.8 M_{\odot}$ and none of our ~ 6000 systems included pairs with a massive component above $1.8 M_{\odot}$ and a low mass component below $1.2 M_{\odot}$, so the highest angular momentum systems are extremely rare.

Although a multitude of dense matter equations of state (EOS) exist which make firm predictions about maximum masses, see for example, Cook et al. (1994), all of them make simplifying assumptions for the physics and theory can not place strong constraints on the final maximum mass. Most models for the neutron star equation of state predict masses in a range between 2.0 and $3.0M_{\odot}$, uncertainties in nuclear physics prevent a more precise prediction of the maximum mass for a non-rotating model. However, for a model with a given maximum non-rotating mass, we can predict the effect of thermal energy and angular momentum.

For our study, we use a variety of equations of state to probe the fate of our merged cores. These include, in particular, the NL3 (Lalazissis et al. 1997) and FSU2.1 (Todd-Rutel and Piekarewicz 2005) EOSs. We also include one of the equation of state models developed in Steiner et al. (2010, 2013, 2015) where the model parameters are matched to observations of quiescent low-mass X-ray binaries and photospheric radius expansion bursts (Steiner et al. 2015) using a Monte Carlo scheme to perform marginal estimation (Steiner et al. 2014b,c). In this equation of state model, matter near and below

the nuclear saturation density is described by a parameterization calibrated to the properties of laboratory nuclei and quantum Monte Carlo simulations (Steiner and Gandolfi 2012). At higher densities, matter is described by two piecewise polytropes. The RNS code for rotating neutron stars from Stergioulas and Friedman (1995) was embedded in our Monte Carlo simulation to output probability distributions for the maximum mass of a neutron star given a fixed angular momentum.

During the merger, shocks and viscous forces increase the energy in the core, raising the entropy. This extra thermal energy can raise the maximum neutron star mass (Kaplan et al. 2014; Bauswein et al. 2014). Most studies where this has been a large effect have assumed entropies of roughly $8 k_B$ per nucleon. However, actual estimates of the post-merger entropies used in our study (Korobkin et al. 2012) lie at about $1 k_B$ per nucleon (Table 1). Using the NL3 (Lalazissis et al. 1997) equation of state (fairly typical) an entropy of $1.28 k_B$ per nucleon raises the maximum stable mass by only 1%. In this scenario, the internal energy deposited in the core in the merged system is not sufficient to strongly affect the maximum neutron star mass. There is more thermal energy in the surrounding disk, but its low densities allow efficient neutrino cooling that is on par with the accretion time. Hence, we will use the accretion time to estimate our collapse rate for systems that collapse after accretion.

The angular momentum in the merged core can, however, have a larger impact on the maximum neutron star mass. If we assume the core quickly evolves into a system in solid body rotation, we can use existing equations of state to estimate the maximum neutron star mass for these rotating systems. For the FSU2.1 equation of state, we find that the maximum neutron star mass increases nearly linearly with rotational support over the range of rotations produced in neutron star mergers (Fig. 2). As input for our population studies, we have fit the maximum neutron star mass predicted for this equation of state with the following linear approximation:

$$M_{\max, \text{NS}} = (2.1 + J/(10^{50} \text{ g cm}^2 \text{ s}^{-1}))M_{\odot} \quad (2)$$

where J is the rotational angular momentum of the compact core. Figure 2 also shows the distortion of the neutron star that would form with such high angular momenta and this distortion reflects the large asymmetries produced in the cores of these merger events.

Thus far we have only used specific equations of state. To determine the role of angular momentum change with a broad range of allowed nuclear equations of state, we use our parameterized equation of state. The increase in the mass (ΔM) of a maximally-rotating neutron star depends upon the maximum mass of the non-rotating neutron star. Figure 3 shows the distribution of ΔM as a function of maximum non-rotating mass. For a $2.0 M_{\odot}$ star, a maximally-rotating neutron star lies between $2.35 - 2.5 M_{\odot}$ depending upon the exact equation of state. For an equation of state producing a maximum non-rotating mass of $2.6 M_{\odot}$, this mass is $3.16 - 3.22 M_{\odot}$, an increase of $0.56 - 0.62 M_{\odot}$. The ΔM for a maximally rotating neutron star increases for equations of state that have larger maximum non-rotating stars. However, for the angular momenta in our merged cores, the increase in

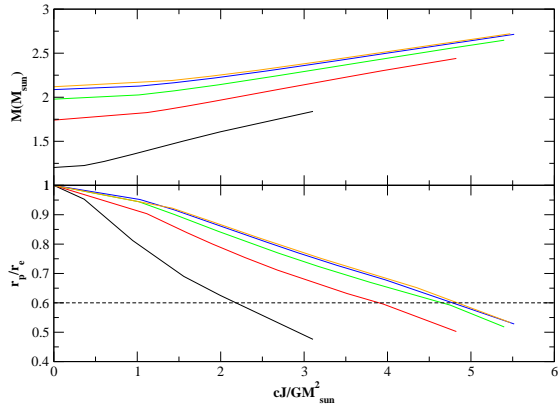


Figure 2. Maximum neutron star mass versus angular momentum for the NL3 equation of state for a set of central pressures (top). A neutron star with a maximum non-rotating mass of $2.1 M_{\odot}$ will have a maximum mass of $2.6 M_{\odot}$. This angular momentum can drastically distort the neutron star. The ratio of the polar to equatorial radii (assuming solid-body rotation) is also shown as a function of angular momentum. At the end of our simulations, the core structure has not yet reached solid body rotation, and the asphericity is even more extreme (possibly arguing for a more extreme maximum mass).

the maximum mass is much less dramatic. A fit to these lower-angular momentum systems yields the following result for the maximum rotating neutron star mass:

$$M_{\text{max,NS}} = M_0 + M_1 \times (J/(10^{49} \text{g cm}^2 \text{s}^{-1}))^{\beta} M_{\odot} \quad (3)$$

where M_0 is the maximum mass for a non-rotating neutron star. For this paper, we study different values of M_0 , fitting the change in mass to average values of rotating systems for a range of angular momenta from $0 - 3 \times 10^{49} \text{g cm}^2 \text{s}^{-1}$ based on the angular momenta in the cores in our simulations (Table 1). For $M_0 = 2.0, 2.5, 2.7 M_{\odot}$, the values for M_1 and β are: $M_1 = 0.0219, 0.0354, 0.0574$ and $\beta = 1.75, 1.5, 1.6$ respectively. Typically, rotation adds less than a few tenths of a solar mass to our maximum mass of our merged cores. Accretion of the disk material can also alter the angular momentum of the core, but how much angular momentum depends upon the exact accretion process (including magnetic field strength). For this study, we assume the specific angular momentum is held constant during the accretion phase. Moreover, we assume that the post-merger magnetic fields are small enough ($B \ll 10^{17} \text{G}$) to not contribute noticeably to the pressure. To obtain a more detailed survey of the possible merger fates, we created a grid of maximum masses, varying M_0 from 2.0 to 2.5 with constant values for M_1 ($= 0.03 M_{\odot}$) and β ($= 1.6$).

With these fits to the maximum mass of our equation of state, we can determine the fate of the merged systems presented in Section 2. Here we use the four fates discussed in Section 2.2: BH, BH_{acc}, BH_{spin}, NS. Note that for these fates, our equation of state models assume that the neutron star has reached an equilibrium density state and it is in solid body rotation. The rotating object is differentially rotating through this period but our simplified assumptions provide an estimate of the importance of spin in the final fate. Spin may prevent an immediate

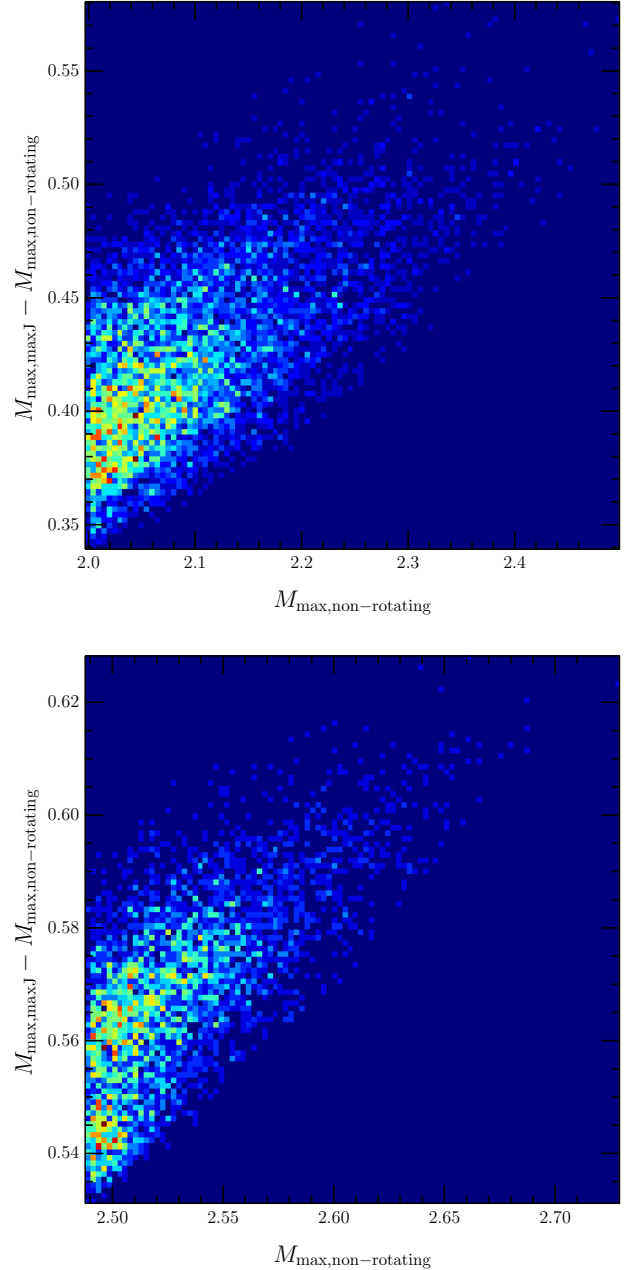


Figure 3. Probability distribution of $\Delta M(M_{\odot})$ as a function of the maximum non-rotating mass. The top panel focuses on masses near and above a maximum mass of $2.0 M_{\odot}$ whereas the bottom panel zooms in on those maximum non-rotating masses above $2.5 M_{\odot}$.

collapse to a black hole but, in most cases, the accretion of the surrounding material is sufficient to cause the core to collapse with or without rotation (see Table 2).

4. TYING IT ALL TOGETHER: POPULATION SYNTHESIS

To compare these results to observations, we must incorporate our findings into a study of the binary neutron star and neutron star/black hole populations. We employ the **StarTrack** population synthesis code (Belczynski et al. 2002, 2008) to generate a population of binary compact objects (in particular NS-NS and BH-NS binaries). The code is based on revised formulas from Hurley et

al. (2000); updated with new wind mass loss prescriptions, calibrated tidal interactions, physical estimation of donor’s binding energy (λ) in common envelope calculations and convection driven, neutrino enhanced supernova engines. A full description of these updates is given in Dominik et al. (2012). The two most recent updates take into account measurements of initial parameter distributions for massive O stars (Sana et al. 2012) as well as a correction of a technical bug that has limited the formation of BH-BH binaries for high metallicity (e.g., $Z = 0.02$).

Two major factors shape the final compact object mass: wind mass loss and core collapse/supernova compact object formation. For wind mass loss we use O/B type winds from Vink et al. (2001) and for other evolutionary stages (e.g., LBV winds) formulae as calibrated in Belczynski et al. (2010). We adopt set of models presented by Fryer et al. (2012) with the rapid core collapse/supernova mechanism. The explosion occurs within the first 0.1–0.2s driven by a convection and neutrino enhanced engine. This “rapid” supernova engine reproduces (Belczynski et al. 2012) the observed mass gap (apparent lack of neutron stars and black holes with mass in range 2–5 M_{\odot}) in Galactic X-ray binaries (Ozel et al. 2010; Bailyn et al. 1998). Additionally, we include NS star formation through electron capture supernovae (ECS) for low mass progenitors $M_{\text{zams}} \sim 7\text{--}11 M_{\odot}$. The range of initial progenitor mass on Zero Age Main Sequence (ZAMS) for ECS depends sensitively on interactions (mass loss and gain) of stars in binary. We assume that all NSs formed through ECS have mass of 1.26 M_{\odot} . Stars initially more massive than $\sim 10 M_{\odot}$ typically form NS in Fe core collapse through our adopted rapid supernova engine. NS are formed in a broad mass range 1.1–2.5 M_{\odot} , although most NSs that form close NS-NS binaries are found in much narrower range 1.2–1.4 M_{\odot} with a long tail extending to 2 M_{\odot} . In our evolutionary calculations we assume that ECS NSs do not receive natal kicks (Podsiadlowski et al. 2004), while for NS formed in Fe core collapse we adopt a 1-D Maxwellian with $\sigma = 265 \text{ km s}^{-1}$ (that corresponds to an average kick of $\sim 400 \text{ km s}^{-1}$ (Hobbs et al. 2005)).

To generate the populations of double compact objects we adopt power-law initial mass function (IMF) with slope of -2.7 for the massive primaries ($M_{\text{zams}} = 5\text{--}150 M_{\odot}$). Secondary mass (less massive binary component) is drawn from flat mass ratio distribution. Then we adopt two very different models for initial orbital separation and eccentricity. In one set of models we adopt flat in logarithm ($\propto 1/a$) distribution of initial separations with thermal eccentricity distribution ($= 2e$). Such assumptions have been adopted in many population synthesis studies (e.g., for references and examples see Belczynski et al. (2008)). We refer to the models employing these assumptions as “OLD”. It was recently pointed out that these distributions may not be adequate for massive progenitors of NSs and BHs. We therefore adopt revised distributions: closer orbital periods $\propto \log(P)^{-0.55}$ and less eccentric orbits $\propto e^{-0.42}$ (Sana et al. 2012). We refer to models with these initial conditions as “NEW”.

Each initial condition calculation is performed for two characteristic stellar metallicities: solar composition $Z = Z_{\odot} = 0.02$ and $Z = 0.1Z_{\odot} = 0.002$. We refer to these

models as high and low-metallicity models. In our mapping of population synthesis calculations with NS-NS merger calculations, we use evenly mixed (50%–50%) population of low and high metallicity models. This is to mimic (in very approximate way) a stellar content of Universe at various redshifts.

In each calculation we allow for a different outcome of Roche lobe overflow (RLOF) initiated by a Hertzsprung gap (HG) donor. If RLOF appears to proceed on a dynamical timescale we perform CE envelope energy calculation to check whether a given binary survives the event (model A). Under this prescription, we allow for the efficient formation of close double compact object binaries. For contrast, we assume that each event of dynamical RLOF with HG donor does not lead to the formation of close double compact object (model B). Some of HG donors (right after main sequence) may not have developed clear core-envelope structure and are a subject to CE merger (e.g., Belczynski et al. (2007)) or at later times HG donors may not have yet developed convective envelope and instead of CE they may potentially initiate thermal-timescale mass transfer that does not allow for significant orbital contraction and close double compact object formation.

Additionally, we allow for uncertainties in our calculation of NS mass. In particular we allow NS mass to increase by a fixed factor and in particular we chose this factor to be 0.1 M_{\odot} . Predictions of neutron star masses fold in a number of uncertainties from understanding the mass of the core at bounce, the duration of the engine phase and the amount of fallback. At the low mass end, fallback is not a concern and the duration of the engine must be short (Fryer et al. 2012). But this initial NS mass can be larger by as much as 0.1 M_{\odot} . In many cases, the first neutron star formed also goes through a common envelope phase where it can accrete up to $\sim 0.1 M_{\odot}$ through hypercritical accretion (Fryer et al. 1996; Belczynski et al. 2002, 2010b; MacLeod & Ramirez-Ruiz 2015,b).

Physical properties of double compact objects of all sorts (NS-NS, BH-NS and BH-BH systems) generated under above conditions are discussed in detail in a series of recent papers Dominik et al. (2012), Dominik et al. (2013), Dominik et al. (2014) and de Mink & Belczynski (2015, to be submitted). The actual population synthesis models are available at www.syntheticuniverse.org. In particular, generated NS-NS merger rates ($\sim 10\text{--}40 \text{ Myr}^{-1}$) are in agreement with the empirically estimated Galactic NS-NS merger rates ($\sim 10\text{--}100 \text{ Myr}^{-1}$; Kim et al. (2015)). The NS masses predicted by our models are in general agreement with the mass estimates available from close NS-NS systems (Fig. 4). However, note that the X-ray binary 4U1538-52 van Kerkwijk et al. (1995) suggests that neutron stars are born with masses below 1.1 M_{\odot} , suggesting the minimum neutron star mass can not be much higher than our standard value, echoing the theoretical error bars of 0.1 M_{\odot} .

With these models, we can determine the fate distributions of merging systems (if and when they form black holes) as a function of the equation of state. Table 3 shows the results for a series of models: with and without systems that undergo a common envelope in the Hertzsprung gap, with the standard initial condi-

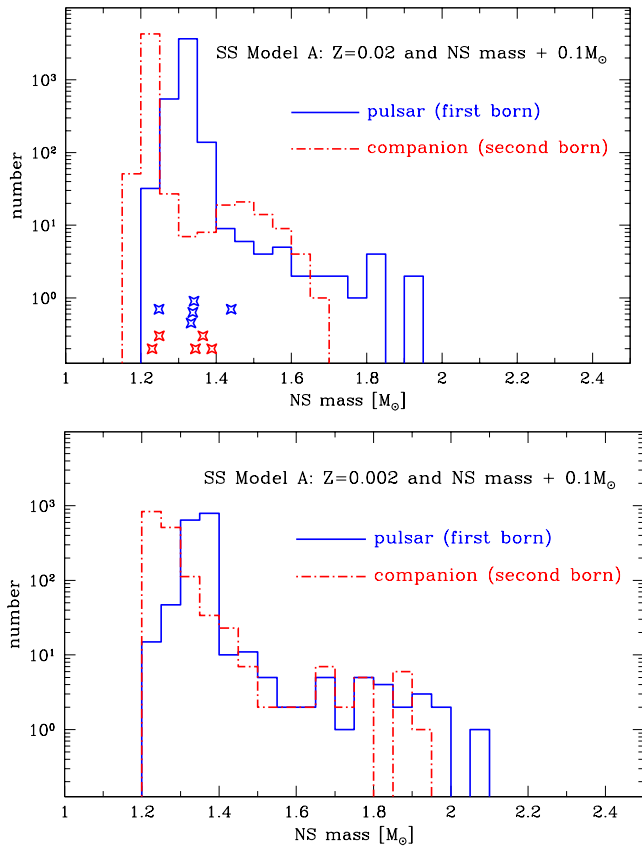


Figure 4. The neutron star mass distribution (number per mass bin as a function of mass) for our models using the “New” initial conditions. These results include systems that have undergone common envelope evolution in the Hertzsprung gap with an enhanced neutron star mass (increasing it by $0.1 M_{\odot}$). For comparison, we plot the masses of the observed NS-NS systems.

tions and the new (Sana et al. 2012) initial conditions, with our standard and modified (increased by $0.1 M_{\odot}$) neutron star masses. The general trends between all these models are the same. The primary fates of the merged binaries are bimodal: either the system collapses to form a black hole after some disk accretion or the core remains a neutron star. Most of the systems that collapse to black holes do so within the first 100 ms. This means that most of the black-hole forming systems could also produce GRBs (avoiding the baryon contamination problem).

The fraction of systems that collapse to a black hole is above 90% for any EOS that has a maximum non-rotating mass below $\sim 2.3\text{-}2.4 M_{\odot}$, but drops precipitously beyond this and most models predict that over 90% of the cores remain neutron stars for any EOS with a higher maximum rotating neutron star. This strong sensitivity to the EOS means that if we can observe these differences, we have a strong probe of the neutron star equation of state. We will discuss the observational implications of these fits in Section 5.

Except at the boundary between most systems forming black holes and most systems forming neutron stars, the differences between the primary fates of our population synthesis models are fairly small (few %). At the boundary, differences in the population of 10% are possible. The primary uncertainty in our calculation is the

lower limit on the neutron star formation mass. For our lower NS formation limit of $1.1 M_{\odot}$, the Steiner2.4 (maximum non-rotating neutron star mass of $2.4 M_{\odot}$) marks the transition between mostly BH final states vs. mostly NS final states. If the mass is increased by $0.1 M_{\odot}$, the Steiner2.5 marks this transition. More importantly for our analysis is the transition EOS for systems that form BHs in less than 100 ms. For these systems, the transition is Steiner2.2, Steiner2.3 respectively for our two mass limits. The other population synthesis parameters do not produce much variation in these results.

5. IMPLICATIONS

In our analysis, we found that the fate of the merged system depends sensitively on the neutron star equation of state. Figure 5 shows the fraction of rapid ($t_{\text{acc}} < 100$ ms) and immediate collapse black holes as a function of the equation of state. If we can observationally distinguish between these fates, we can use NS-NS mergers to place constraints on the equation of state.

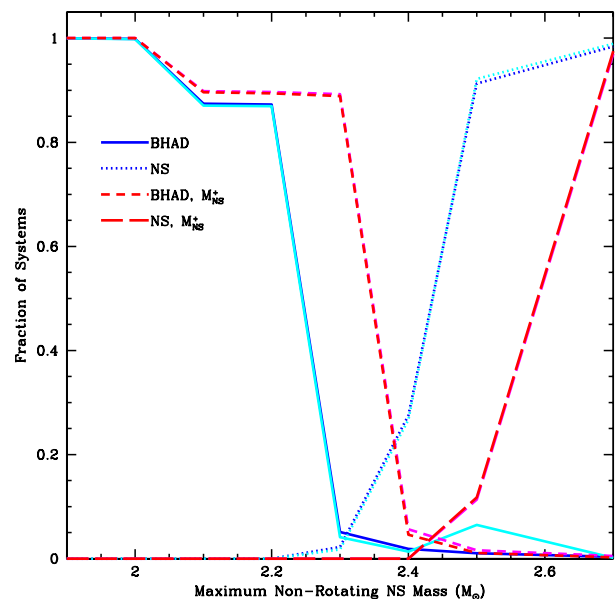


Figure 5. Fraction of systems that produce standard BHAD GRBs and Neutron stars for our 4 basic population models: standard NS masses (BHAD - solid, NS - dotted) for old (blue) and new (cyan) initial orbital parameters, NS masses increased by $0.1 M_{\odot}$ (BHAD - dashed, NS - long-dashed) for old (red) and new (magenta) initial orbital conditions. The orbital conditions have virtually no effect on these results and the variations caused by other binary population synthesis parameters is also negligible. The primary error in these estimates is that of the initial mass distribution of neutron stars, producing an equivalent error in the maximum non-rotating NS mass limit on the EOS.

For example, the current favored model for short-duration GRBs is the merger of two neutron stars forming a black hole accretion disk. If the merged core forms a neutron star, neutrino-driven winds (Dessart et al. 2009; Perego et al. 2014) drive outflows through which any jet must penetrate to produce a gamma-ray burst. Current studies argue that this well-known baryon contamination problem can only be avoided if the neutron star phase lasts less than ~ 100 ms (Murguía-Berthier et al. 2014).

If this is true, GRBs are produced in only a fraction of all merging systems. If the maximum mass is below $2.3\text{-}2.4 M_{\odot}$, then the cores of most neutron star mergers produce black holes within ~ 100 ms of the merger. For these equations of state, most neutron star mergers are capable of forming short-duration GRBs.

Above a maximum non-rotating neutron star mass of $2.3\text{-}2.4 M_{\odot}$, less than 4% of all mergers produce rapid-collapse black hole systems within 100 ms. If only such black hole systems form short-duration GRBs, this would require a rate of mergers that is 50 times higher than canonical values. Although possible, this strains our current understanding of binary and stellar evolution, arguing strongly that the maximum neutron star mass is below $2.3\text{-}2.4 M_{\odot}$. Advanced LIGO will be able to place more stringent constraints on this merger rate, and this measured merger rate will provide more firm constraints on the maximum neutron star mass.

Unfortunately, constraining the NS-NS merger rate and its comparison with short GRB rates may not directly constrain the equation of state. BH-NS mergers can also produce short-duration GRBs and, in a small subset of binary population synthesis scenarios, BH-NS merger rate is on par with the NS-NS merger rate, e.g. (Dominik et al. 2012). Although it is possible to construct a scenario where BH-NS mergers dominate the rate of NS-NS mergers, recall from Section 2.1 that it is likely that most of BH-NS systems do not produce disks of sufficient size to make GRBs (Rosswog 2015). If the connection between the short GRBs and BH-NS mergers could be established, it will place strong constraints on binary population synthesis models (in most scenarios, the NS-NS merger rate is an order of magnitude higher than the BH-NS merger rate; Dominik et al. (2012). It will also point to the EOS with maximum NS mass over $2.3\text{-}2.4 M_{\odot}$ as such EOS allows to eliminate the formation of short GRBs from NS-NS mergers via most accepted (BHAD) engine model.

Alternatively, it is possible that the baryon loading from neutrino-driven winds from neutron stars does not preclude the possibility that cores that remain neutron stars can produce GRBs. Late-time emission from short-duration GRBs either argues for some extended power source (e.g. late-time accretion, magnetar) or jet interaction (Holcomb et al. 2014). The magnetar power source requires a long-lived neutron star and has been shown, within the free parameters of the magnetar model (Rowlinson et al. 2014), to fit the late-time emission well. Proponents of the magnetar model argue that there must be some way to avoid the burying of the magnetic field and the baryon loading, e.g. a high pressure, magnetic or radiation dominated, region along the axis prevents baryon loading and allows the production of a relativistic jet.

To rule out these alternative solutions, we either need to refine our theoretical models to prove the differences in the current interpretations or we need additional observational diagnostics to distinguish the above picture. For example, it might be possible to distinguish BH from NS formation using the gravitational wave signal (Chatziioannou et al. 2015), but this will likely require a very strong signal from a nearby merger. If a stable neutron star with strong magnetic fields is formed, we would expect continued pulsar-like activity, e.g. a soft gamma-ray repeater. However, if we only have LIGO localizations,

it will be difficult to prove the association of any activity with the merger, e.g. (Kelley et al. 2010). The ejecta from these models could allow us to distinguish these models. The optical/infra-red light produced by the decay of radioactive elements can be used to distinguish between NS and BH fates. The masses of the dynamic ejecta that are shown in figure 6) do not vary dramatically in our models and, without alteration by the core, the extreme neutron-richness of these ejecta leads to a composition that almost exclusively consists of very massive nuclei with very large opacities (Kasen et al. 2013) producing transients peaking in the near-infrared (or infrared) (Roberts et al. 2011; Barnes & Kasen 2013; Tanaka & Hotokezaka 2013; Grossman et al. 2014; Fontes et al. 2015). However, the transient observed post-merger is composed of emission produced by a combination of this dynamic ejecta, neutrino driven winds from the core (if the core does not collapse to a black hole) and ejecta from the disk accretion. Due to the longer exposure to the intense neutrino background, the neutron fraction is reduced, altering the composition of these ejecta and the revised opacities may allow brighter transients in the near-infrared and optical (Perego et al. 2014). Since this ejecta is much larger for NS systems than BH disk systems (Fernandez et al. 2015; Just et al. 2015), we may be able to distinguish these two systems by the wavelength of their electromagnetic emission. If so, we can use observations of neutron star mergers to place constraints on dense matter equations of state.

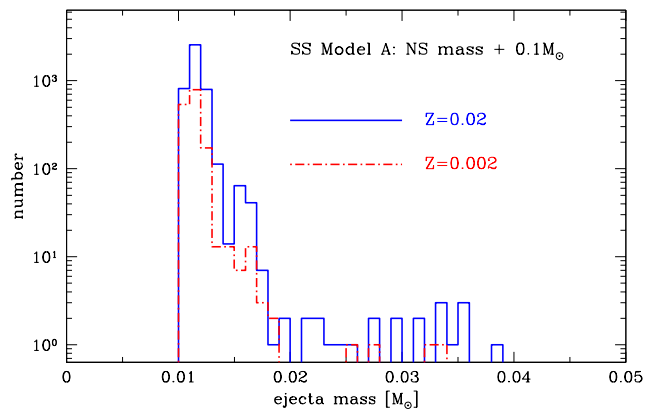


Figure 6. The number of systems as function of ejecta mass in the tidal tails from these neutron star mergers for our increased NS models for both solar and 1/10th solar metallicity. Note that although the ejecta masses range from below $0.01 M_{\odot}$ to above $0.03 M_{\odot}$, 75% of the mergers produce ejecta with masses of $0.025 \pm 0.003 M_{\odot}$.

Acknowledgments This project was funded in part under the auspices of the U.S. Dept. of Energy, and supported by its contract W-7405-ENG-36 to Los Alamos National Laboratory. KB acknowledges support from the Polish Science Foundation “Master2013” subsidy and by the Polish NCN grant SANATA BIS. This project originated at a KITP workshop supported by NSF Grant No. PHY11-25915. This work was supported in part by the Simons Foundation and the hospitality of the Aspen Center for Physics. The rotating neutron star simulations used computational resources from the University of Tennessee and Oak Ridge National Laboratory’s Joint

Institute for Computational Sciences.

REFERENCES

- Antoniadis, J., Freire, P.C.C., Wex, N., Tauris, T.M., Lynch, R.S., *et al.* 2013, *Science*, 340 1233232
- Banres, J., Kasen, D. 2013, 775, 18
- Bauswein, A., Baumgarte, T.W., Janka, H.-T. 2014, *Phys. Rev. Lett.*, 111, 131101
- Bauswein, A., Stergioulas, N., Janka, H.-T. 2014, *Phys. Rev. D*, 90, 023002
- Behroozi, P.S., Ramirez-Ruiz, E., Fryer, C.L. 2014, *astro-ph/1401.7986*
- Bailyn, C.D., Jain, R.K., Coppi, P., Orosz, J.A. 1998, *ApJ*, 499, 367
- Belczynski, K., Kalogera, V., Bulik, T. 2002, *ApJ*, 572, 407
- Belczynski, K., Perna, R., Bulik, T., Kalogera, V., Ivanova, N., Lamb, D. Q. 2002, *ApJ*, 572, 407
- Belczynski, K., Taam, R.E., Kalogera, V., Rasio, F.A., Bulik, T. 2007, *ApJ*, 662, 504
- Belczynski, K., Taam, R.E., Rantsiou, E., van der Sluys, M. 2008, *ApJ*, 682, 474
- Belczynski, K., Rasio, F.A., Taam, R.E., Zezas, A., Bulik, T., Maccarone, T.J., Ivanova, N. 2008, *ApJ*, 174, 223
- Belczynski, K., Dominik, M., Bulik, T., O’Shaughnessy, R., Fryer, C., Holz, D.E. 2010, *ApJ*, 715, L138
- Belczynski, K., Lorimer, D.R., Ridley, J.P., Curran, S.J. 2010, *MNRAS*, 407, 1245
- Belczynski, K., Wiktorowicz, G., Fryer, C.L., Holz, D.E., Kalogera, V. 2012, *ApJ*, 757, 91
- Berger, E. 2014, *ARA&A*, 52, 43
- Bildsten, L., Cutler, C. 1992, *ApJ*, 400, 175
- Bloom, J.S., Sigurdsson, S., Pols, O.R. 1999, *MNRAS*, 305, 763
- Chatziioannou, K., Cornish, N., Klein, A., Yunes, N. 2015, *ApJ*, 798, 17
- Cook, G.B., Shapiro, S.L., Teukolsky, S.A. 1994, *ApJ*, 424, 823
- Demorest, P.B., Pennucci, T., Ransom, S.M., Roberts, M.S.E., Hessels, J.W.T. 2010, 467, 1081
- Dessart, L., Ott, C. D., Burrows, A., Rosswog, S., and Livne, E. 2009, *ApJ*, 690, 1681
- Dominik, M., Belczynski, K., Fryer, C., Holz, D.E., Berti, E., Bulik, T., Mandel, I., O’Shaughnessy, R., *ApJ*, 759, 52
- Dominik, M., Belczynski, K., Fryer, C., Holz, D.E., Berti, E., Bulik, T., Mandel, I., O’Shaughnessy, R., *ApJ*, 779, 72
- Dominik, M., Berti, E., O’Shaughnessy, R., Belczynski, K., Fryer, C., Holz, D.E., Bulik, T., Pannarale, F., *astro-ph/1405.7016*
- Duncan, R.C. and Thompson, C. 1992, *ApJ*, 392, L9
- East, W.E., McWilliams, S.T., Levin, J., Pretorius, F. 2013, *Phys. Rev. D*, 87, 043004
- Fernandez, R., Quataert, E., Schwab, J., Kasen, D., Rosswog, S. 2015, *MNRAS*, 449, 390
- Fong, W., Berger, E. 2013, *ApJ*, 776, 18
- Fontes, C.J., in preparation
- Foucart, F., Duez, M. D., Kidder, L. E., Teukolsky, S. A. 2010, *astro-ph/1007.4203*.
- Foucart, F., Duez, M. D., Kidder, L. E., Scheel, M. A., Szilagyi, G., Teukolsky, S. A. 2011, *PRD*, 85, 044015
- Foucart, F. 2012, *PRD*, 86, 124007
- Foucart, F., O’Connor, E., Roberts, L., Duez, M. D., Haas, R., Kidder, L. E., Ott, C. D., Pfeiffer, H. P., Scheel, M. A., Szilagyi, G., Teukolsky, S. A. 2015, *astro-ph/1502.04146*
- Fryer, C.L., Benz, W., Herant, M. 1996, *ApJ*, 460, 801
- Fryer, C.L., Woosley, S.E., & Hartmann, D.H. *ApJ*, 526, 152
- Fryer, C.L., Belczynski, K., Wiktorowicz, G., Dominik, M., Kalogera, V., Holz, D.E. 2012, *ApJ*, 749, 91
- Grindlay, J., Portegies-Zwart, S., McMillan, S. *Nature*, 2, 116
- Grossman, D., Korobkin, O., Rosswog, S., Piran, T. 2014, *MNRAS*, 439, 757
- Hobbs, G., Lorimer, D.R., Lyne, A.G., Kramer, M. 2005, *MNRAS*, 360, 974
- Hotkezaka, K., Kiuchi, K., Kyutoku, K., Muranushi, T., Sekiguchi, Y.-I., Shibata, M., Taniguchi, K. 2013, *PRD*, 88, 044026
- Holcomb, C., Ramirez-Ruiz, E., De Colle, F., Montes, G. 2014, *ApJ*, 790, L3
- Houck, J.C., Chevalier, R.A. 1991, *ApJ*, 376, 234
- Hurley, J.R., Pols, O.R., Tout, C.A. 2000, *MNRAS*, 315, 543
- Just, O., Bauswein, A., Pulpillo, R. A., Goriely, S., Janka, H.-T. 2015, *MNRAS*, 448, 541
- Kasen, D., Badnell, N. R., Barnes, J. 2013, *ApJ*, 774, 25
- Kelley, L.Z., Ramirez-Ruiz, E., Zemp, M., Diemand, J., Mandel, I. 2010, *ApJ*, 752, L91
- Kim, C., Perera, B.B.P., and McLaughlin, M.A. 2015, *MNRAS*, 448, 928
- Kiuchi, K., Kyutoku, K., Sekiguchi, Y., Shibata, M., Wada, T. 2014, *Phys. Rev. D.*, 90, 041502
- Kaplan, J.D., Ott, C.D., O’Connor, E.P., Kiuchi, K., Roberts, L., and Duez, M. 2014, *ApJ*, 790, 19
- Klebesadel, R.W., & Strong, I.B., *Ap&SS*, 42, 3
- Kochanek, C.S. 1992, *ApJ*, 398, 234
- Korobkin, O., Rosswog, S., Arcones, A., Winteler, C. 2012, *ApJ*, 426, 1940
- Kouveliotou, C., *et al.* 1993, *ApJ*, 413, L101
- kyutoku, K., Ioka, K., Shibata, M. 2013, *astro-ph/1305.6309*
- Lalazissis, G.A., Konig, J., and Ring, P. 1997, *PRC*, 55, 540
- Lee, W. H., and Ramirez-Ruiz, E. 2007, *NJPh*, 9, 17
- Lee, W. H., Ramirez-Ruiz, E., López-Cámara, D. 2009, *ApJ*, 699, L93
- Lee, W. H., Ramirez-Ruiz, E., van de Ven, G. 2010, *ApJ*, 720, 953
- Macleod, M., Ramirez-Ruiz, E. 2015, *ApJ*, 798, L19
- Macleod, M., Ramirez-Ruiz, E. 2015, *ApJ*, 803, 41
- Murguia-Berthier, A., Montes, G., Ramirez-Ruiz, E., DeColle, F., Lee, W.H. 2014, *ApJ*, 788, L8
- Özel, F., Psaltis, D., Narayan, R., McClintock, J.E. 2010, *ApJ*, 725, 1918
- Paschalidis, V., Ruiz, M., Shapiro, S.L. 2014, *astro-ph/1410.7392*
- Perego, A., Rosswog, S., Cabezón, R. M., Korobkin, O., Käppeli, R., Arcones, A., Liebendörfer, M. 2014, *MNRAS*, 443, 3134
- Podsiadlowski, P., Langer, N., Poelarends, J.J.T., Rappaport, S., Heger, A., Pfahl, E. 2004, *ApJ*, 612, 1044
- Popov, S.B., Turolla, R. 2012 *Electromagnetic Radiation from pulsars and Magnetars. Proceedings of a Conference held at University of Zielona Góra, Zielona Góra, Poland, 24-27 April 2012, San Francisco: Astronomical Society of the Pacific, 466, 191*
- Popham, R., Woosley, S.E., Fryer, C., *ApJ*, 518, 356
- Radice, D., Rezzolla, L., Galeazzi, F. 2014, *Clas. and Quant. Gravity*, 31, 075012
- Ramirez-Ruiz, E., Trenti, M., MacLeod, M., Roberts, L.F., Lee, W.H., Saladino-Rosas, M.I. 2015, *ApJ*, 802, L22
- Rantsiou, E., Kobayashi, S., Laguna, P., Rasio, F.A., *ApJ*, 680, 1326
- Roberts, L.F., Kasen, D., Lee, W.H., Ramirez-Ruiz, E. 2011, *ApJ*, 736, L21
- Rosswog, S., & Davies, M.B. 2002, *MNRAS*, 334, 481
- Rosswog, S., & Ramirez-Ruiz, E. 2002, *MNRAS*, 336, L7
- Rosswog, S., Ramirez-Ruiz, E., & Davies, M.B. 2003, *MNRAS*, 345, 1077
- Rosswog, S., Speith, R., Wynn, G.A. 2004, *MNRAS*, 351, 1121
- Rosswog, S. 2005, *ApJ*, 634, 1202
- Rosswog, S., Piran, T., Nakar, E. 2013, *MNRAS*, 430, 2585
- Rosswog, S. 2015, *IJMPD*, 24, 1530012
- Rowlinson, A., Gompertz, B.P., Dainotti, M., O’Brien, P.T., Wijers, R.A.M.J., van der Horst, A.J. 2014, *ApJ*, 43, 1779
- Sana, H., de Mink, S.E., de Koter, A., Langer, N., Evans, C.J., Giele, M., Gosset, E., Izzard, R.G., Le Bouquin, J.-B., Schneider, F.R.N. 2012, *Science*, 337, 444
- Shibata, M., Sekiguchi, Y.-I., Takahashi, R. 2007, *Progress of Theoretical Physics*, 118, 257
- Shibata, M., Taniguchi, K., Okawa, H., Buonanno, A. 2014, *Phys. Rev. D.*, 89, 084005
- Steiner, A.W., Lattimer, J.M., Brown, E.F. 2010, *ApJ*, 722, 33
- Steiner, A.W. and Gandolfi, S. 2012, *PRL*, 108, 088102
- Steiner, A.W., Lattimer, J.M., Brown, E.F. 2013, *ApJ*, 765, L5
- Steiner, A.W., Gandolfi, S., Fattoyev, F.J., Newton, W.G. 2015, *PRC*, 91, 015804
- Steiner, A.W. 2014, *O₂scl*, Astrophysics Source Code Library, record ascl:1408.019
- Steiner, A.W. 2014, *Bamr*, Astrophysics Source Code Library, record ascl:1408.020
- Stergioulas, N. and Friedman, J.L. 1995, *ApJ*, 444, 306.

Table 1
Merger Properties^a

M_{NS1} (M_{\odot})	M_{NS2} (M_{\odot})	$M_{\text{core}}^{\text{b}}$ (M_{\odot})	$S_{\text{core}}^{\text{b}}$ (kB/nuc)	$J_{\text{core}}^{\text{b}}$ ($10^{49}\text{gcm}^2\text{s}^{-1}$)	$M_{\text{disk}}^{\text{b}}$ (M_{\odot})	$M_{\text{ejected}}^{\text{b}}$ (M_{\odot})	$r_{\text{equator}}^{\text{c}}$ (km)	$r_{\text{pole}}^{\text{c}}$ (km)
1.0	1.0	1.51	0.91	1.43	0.48	0.0084	21.3	10.9
1.2	1.0	1.58	0.93	1.12	0.59	0.029	20.9	12.9
1.4	1.0	1.74	0.94	1.22	0.63	0.028	21.9	13.5
1.6	1.0	1.86	1.07	1.20	0.71	0.030	18.2	13.6
1.8	1.0	2.10	1.06	2.27	0.67	0.032	71.1	14.2 ^d
2.0	1.0	2.14	1.28	1.41	0.83	0.032	175.3	14.4 ^d
1.2	1.2	1.87	0.94	1.91	0.52	0.010	22.4	12.6
1.4	1.2	2.01	0.95	1.92	0.57	0.022	24.0	13.4
1.6	1.2	2.10	0.97	1.88	0.67	0.034	23.2	14.0
1.8	1.2	2.19	1.19	1.87	0.77	0.036	21.9	14.9
2.0	1.2	2.31	1.43	1.89	0.85	0.037	73.5	14.6 ^d
1.3	1.4	2.08	1.01	2.22	0.61	0.016	21.6	12.7
1.3	1.4 ^e	2.02	0.69	1.86	0.67	0.016	20.6	12.9
1.4	1.4	2.29	0.96	3.11	0.50	0.012	25.2	11.6
1.6	1.4	2.33	0.95	2.41	0.65	0.021	25.4	13.9
1.8	1.4	2.40	1.00	2.15	0.76	0.038	25.2	14.3
2.0	1.4	2.48	1.45	2.15	0.88	0.041	25.4	14.7
1.6	1.6	2.55	1.03	3.07	0.64	0.013	23.7	13.6
1.8	1.6	2.71	1.08	3.36	0.67	0.019	25.2	13.8
2.0	1.6	2.70	1.36	2.76	0.86	0.042	24.5	14.6
1.8	1.8	2.87	1.08	3.84	0.71	0.015	25.9	13.6
2.0	1.8	3.04	1.28	4.11	0.74	0.019	26.4	14.2
2.0	2.0	3.31	1.19	5.37	0.67	0.017	14.1	13.3

^a All models from (Korobkin et al. 2012) with the simulation physics from (Rosswog 2013).

^b The core is defined by the post-merger material whose density is above 10^{14}gcm^{-3} at the end of the calculation.

^c $r_{\text{pole}}, r_{\text{equator}}$ correspond to the radius of the compact core along the rotation axis and equator respectively assuming the core reaches a uniformly-rotating, equilibrium state using the FSU2.1 equation of state.

^d For the most part, the angular momenta in these proto-neutron star is just below most limits for secular instabilities. For these 3 systems, this is not the case. It is possible that these instabilities can quickly shed angular momentum.

^e This model assumes co-rotation for the initial conditions.

Takami, K., Rezzolla, L., Baiotti, L. 2014, Phys. Rev. Lett., 113, 091104

Tanaka, M., Hotokezaka, K. 2013, ApJ, 775, 113

Thompson, C. MNRAS, 270, 480

Todd-Rutel, B.G. and Piekarewicz, J. 2005, PRL, 95, 122501

Tsang, D. 2013, ApJ, 777, 103

Usov, V.,V. 1992, Nature, 357, 472

van Kerkwijk, M.H., van Paradijs, J., and Zuiderwijk, E.J. Astron. Astrophys., 303, 495 (1995)

Vigano, D., Pons, J.A. 2012, MNRAS, 425, 2487

Vink, J.S., de Koter, A., Lamers, H.J.G.L.M. 2001, A&A, 369, 574

Woosley, S.E., ApJ, 411, 823

Zemp, M., Ramirez-Ruiz, E., Diemand, J. ApJ, 705, L186

Zhang, B., and Meszaros, P. 2001, ApJ, 552, L35

Table 2
Remnant Fate

M_{NS1} (M_{\odot})	M_{NS2} (M_{\odot})	Fate (eq.2) ^a FSU2.1	Fate (eq.3) ^a $M_0 = 2.0$	Fate (eq.3) ^a $M_0 = 2.2$	Fate (eq.3) ^a $M_0 = 2.3$	Fate (eq.3) ^a $M_0 = 2.4$	Fate (eq.3) ^a $M_0 = 2.5$	Fate (eq.3) ^a $M_0 = 2.7$
1.0	1.0	NS	NS	NS	NS	NS	NS	NS
1.2	1.0	BH _{spin}	BH _{acc} : 210	NS	NS	NS	NS	NS
1.4	1.0	BH _{acc} : 180	BH _{acc} : 40	BH _{acc} : 220	BH _{acc} : 1.2s	NS	NS	NS
1.6	1.0	BH _{acc} : 90	BH _{acc} : 90	BH _{acc} : 90	BH _{acc} : 100	BH _{acc} : 240	BH _{acc} : 1.8s	NS
1.8	1.0	BH _{acc} : 60	BH	BH _{acc} : 20	BH _{acc} : 90	BH _{acc} : 120	BH _{acc} : 360	BH _{spin}
1.8	1.0 ^b	BH	BH	BH	BH	90	200	BH _{spin}
2.0	1.0	BH _{acc} : 50	BH	BH	BH _{acc} : 50	BH _{acc} : 50	BH _{acc} : 50 (BH)	BH _{acc} : 170
2.0	1.0 ^b	BH	BH	BH	BH	BH	BH	90
1.2	1.2	BH _{acc} : 500	BH _{acc} : 50	BH _{acc} : 450	BH _{acc} : > 3s	NS	NS	NS
1.4	1.2	BH _{acc} : 50	BH	BH _{acc} : 50	BH _{acc} : 280	BH _{acc} : 480	BH _{spin}	NS
1.6	1.2	BH _{acc} : 10	BH	BH _{acc} : 20	BH _{acc} : 30	BH _{acc} : 70	BH _{acc} : 200	BH _{spin}
1.8	1.2	BH _{acc} : 10	BH	BH _{acc} : 20	BH _{acc} : 30	BH _{acc} : 30	BH _{acc} : 30	BH _{acc} : 200
2.0	1.2	BH	BH	BH	BH	BH	BH _{acc} : 60	BH _{acc} : 60
2.0	1.2 ^b	BH	BH	BH	BH	BH	BH	BH _{acc} : 30
1.3	1.4	BH _{acc} : 60	BH _{acc} : 60	BH _{acc} : 60	BH _{acc} : 70	BH _{acc} : 300	BH _{acc} : > 3s	NS
1.3	1.4 ^c	BH _{acc} : ~ 3s	BH _{acc} : ~ 3s	BH _{acc} : ~ 3s	BH _{acc} : ~ 3s	BH _{acc} : ~ 3s	BH _{acc} : ~ 3s	NS
1.4	1.4	BH _{acc} : 60	BH	BH _{acc} : 60	BH _{acc} : 60	BH _{acc} : 60	BH _{acc} : 490	BH _{spin}
1.6	1.4	BH	BH	BH	BH	BH _{acc} : 30	BH _{acc} : 60	BH _{acc} : 700
1.8	1.4	BH	BH	BH	BH	BH _{acc} : 20	BH _{acc} : 40	BH _{acc} : 80
2.0	1.4	BH	BH	BH	BH	BH	BH _{acc} : 40	BH _{acc} : 40
1.6	1.6	BH	BH	BH	BH	BH	BH _{acc} : 30	BH _{acc} : 420
1.8	1.6	BH	BH	BH	BH	BH	BH _{acc} : 40	BH _{acc} : 130
2.0	1.6	BH	BH	BH	BH	BH	BH	BH _{acc} : 50
1.8	1.8	BH	BH	BH	BH	BH	BH	BH _{acc} : 70
2.0	1.8	BH	BH	BH	BH	BH	BH	BH _{acc} : 30
2.0	2.0	BH	BH	BH	BH	BH	BH	BH _{acc} : 40

^a The final fates are NS, the merged system forms a NSAD that, even after the accretion of a disk, remains a NS; BH_{acc}, merged system initially forms a NSAD that, after some accretion, collapses to a BH forming a BHAD (the accretion time is given in ms unless otherwise specified); BH_{spin}, merged system initially forms a NSAD that only collapses after the disk accretion and the loss of angular momentum; BH, the merged system collapses immediately to a BH, forming a BHAD; BH_{spin} (the merged system remains a NSAD until the disk accretion finishes after which spin down is able to decrease the maximum neutron star mass and allow it to collapse to a black hole.)

^b For these models, we consider the fate of the neutron star with a reduced rotation assuming the secular instabilities quickly reduce the angular momentum. Any changes are noted in parantheses. Note, however, that typical growth timescales for these systems are estimated to be above 100 ms and it is more likely that the spin down occurs after the accretion phase.

^c This model assumes co-rotation for the initial conditions.

Table 3
Merger Fate Distributions^a

Equation of State ^b	BHAD GRB ^a	BH ^a	BH _{acc} , $t_{\text{acc}} < 100\text{ms}$ ^a	BH _{acc} , $t_{\text{acc}} > 100\text{ms}$ ^a	BH _{spin} ^a	NS ^a
FSU2.1 ^c	0.8739 (0.8715)	0.0106 (0.0100)	0.8633 (0.8615)	0.1211 (0.1259)	0.0051 (0.0026)	0.0000 (0.0000)
Steiner2.0	0.9988 (1.0000)	0.8730 (0.8707)	0.1258 (0.1293)	0.0012 (0.0000)	0.0000 (0.0000)	0.0000 (0.0000)
Steiner2.2	0.8723 (0.8707)	0.0090 (0.0091)	0.8633 (0.8615)	0.1209 (0.1259)	0.0067 (0.0035)	0.0000 (0.0000)
Steiner2.3	0.0510 (0.0786)	0.0104 (0.0095)	0.0406 (0.0690)	0.8734 (0.9010)	0.0532 (0.0139)	0.0224 (0.0065)
Steiner2.4	0.0189 (0.0113)	0.0066 (0.0087)	0.0123 (0.0026)	0.1514 (0.0924)	0.5543 (0.4952)	0.2754 (0.4010)
Steiner2.5	0.0104 (0.0095)	0.0032 (0.0048)	0.0072 (0.0048)	0.0104 (0.0013)	0.0671 (0.0694)	0.9120 (0.9197)
Steiner2.7	0.0034 (0.0048)	0.0000 (0.0000)	0.0034 (0.0048)	0.0057 (0.0048)	0.0072 (0.0009)	0.9838 (0.9896)
FSU2.1 ^d	0.8704 (0.8662)	0.0065 (0.0040)	0.8639 (0.8622)	0.1248 (0.1323)	0.0048 (0.0015)	0.0000 (0.0000)
Steiner2.0	0.9982 (1.0000)	0.8690 (0.8642)	0.1291 (0.1358)	0.0018 (0.0000)	0.0000 (0.0000)	0.0000 (0.0000)
Steiner2.2	0.8694 (0.8662)	0.0055 (0.0040)	0.8639 (0.8622)	0.1253 (0.1319)	0.0053 (0.0020)	0.0000 (0.0000)
Steiner2.3	0.0414 (0.0652)	0.0063 (0.0040)	0.0351 (0.0612)	0.8839 (0.9210)	0.0568 (0.0094)	0.0179 (0.0044)
Steiner2.4	0.0134 (0.0074)	0.0040 (0.0040)	0.0094 (0.0035)	0.1587 (0.0785)	0.5610 (0.5042)	0.2669 (0.4099)
Steiner2.5	0.0065 (0.0040)	0.0012 (0.0010)	0.0053 (0.0030)	0.0087 (0.0015)	0.0631 (0.0612)	0.9217 (0.9333)
Steiner2.7	0.0015 (0.0005)	0.0000 (0.0000)	0.0015 (0.0005)	0.0042 (0.0035)	0.0052 (0.0010)	0.9891 (0.9951)
FSU2.1 ^e	0.8981 (0.8724)	0.0159 (0.0100)	0.8821 (0.8624)	0.1019 (0.1276)	0.0000 (0.0000)	0.0000 (0.0000)
Steiner2.0	1.0000 (1.0000)	0.8851 (0.8355)	0.1149 (0.1645)	0.0000 (0.0000)	0.0000 (0.0000)	0.0000 (0.0000)
Steiner2.2	0.8964 (0.8724)	0.0144 (0.0100)	0.8820 (0.8624)	0.1036 (0.1276)	0.0000 (0.0000)	0.0000 (0.0000)
Steiner2.3	0.8923 (0.8724)	0.0149 (0.0100)	0.8774 (0.8624)	0.1077 (0.1276)	0.0000 (0.0000)	0.0000 (0.0000)
Steiner2.4	0.0566 (0.0799)	0.0107 (0.0087)	0.0458 (0.0712)	0.8726 (0.8655)	0.0708 (0.0547)	0.0000 (0.0000)
Steiner2.5	0.0159 (0.0100)	0.0055 (0.0074)	0.0104 (0.0026)	0.0523 (0.0438)	0.8182 (0.7947)	0.1136 (0.1515)
Steiner2.7	0.0052 (0.0078)	0.0000 (0.0000)	0.0052 (0.0078)	0.0086 (0.0022)	0.0164 (0.0039)	0.9698 (0.9861)
FSU2.1 ^f	0.8961 (0.8667)	0.0107 (0.0044)	0.8854 (0.8622)	0.1039 (0.1333)	0.0000 (0.0000)	0.0000 (0.0000)
Steiner2.0	1.0000 (1.0000)	0.8839 (0.8326)	0.1161 (0.1674)	0.0000 (0.0000)	0.0000 (0.0000)	0.0000 (0.0000)
Steiner2.2	0.8938 (0.8667)	0.0085 (0.0044)	0.8853 (0.8622)	0.1062 (0.1333)	0.0000 (0.0000)	0.0000 (0.0000)
Steiner2.3	0.8886 (0.8662)	0.0100 (0.0040)	0.8786 (0.8622)	0.1114 (0.1338)	0.0000 (0.0000)	0.0000 (0.0000)
Steiner2.4	0.0459 (0.0652)	0.0062 (0.0044)	0.0398 (0.0607)	0.8806 (0.8785)	0.0735 (0.0563)	0.0000 (0.0000)
Steiner2.5	0.0107 (0.0044)	0.0038 (0.0030)	0.0068 (0.0015)	0.0478 (0.0360)	0.8240 (0.7985)	0.1176 (0.1610)
Steiner2.7	0.0023 (0.0020)	0.0000 (0.0000)	0.0023 (0.0020)	0.0058 (0.0025)	0.0167 (0.0049)	0.9751 (0.9906)

^a We include 4 suites of simulations corresponding two different initial conditions: standard/old StarTrak initial conditions (Belczynski et al. 2008) and the new initial conditions (Sana et al. 2012) and two different initial compact remnant mass distributions. For each result, we include two values, one where all systems are included and one where it is assumed that the binary is destroyed if the system goes through a common envelope in the Hertzsprung Gap. For the remnant fates, we consider those systems that collapse immediately (within 3 ms of the merger) to a BH (BH), systems that collapse to a BH within 100 ms ($\text{BH}_{\text{acc}}, t_{\text{acc}} < 100\text{ms}$), those that collapse to a BH through accretion taking more than 100 ms ($\text{BH}_{\text{acc}}, t_{\text{acc}} > 100\text{ms}$), those that collapse only after spin-down (BH_{spin}), and those that remain neutron stars (NS). The first column is the sum of the second and third columns (BH+BH_{acc}, $t_{\text{acc}} < 100\text{ms}$) and represents those systems that can form the canonical black hole accretion disk GRB without significant baryonic contamination.

^b The equations of state correspond to the FSU2.1 equation of state with a maximum non-rotating neutron star mass of $2.1 M_{\odot}$ and a range of equations of state from our parameterized model (SteinerX) where “X” denotes the maximum non-rotating neutron star mass for that equation of state (in M_{\odot}).

^c This suite studies the old initial conditions with the standard NS mass distribution.

^d This suite studies the new conditions with the standard NS mass distribution.

^e This suite studies the old initial conditions with the enhanced ($+0.1 M_{\odot}$) NS mass distribution.

^f This suite studies the new new conditions with the enhanced ($+0.1 M_{\odot}$) NS mass distribution.